

LQR and SMC Stabilization of a New Unmanned Aerial Vehicle

Kaan T. Oner, Ertugrul Cetinsoy, Efe Sirimoglu, Cevdet Hancer, Taylan Ayken, and Mustafa Unel

Abstract—We present our ongoing work on the development of a new quadrotor aerial vehicle which has a tilt-wing mechanism. The vehicle is capable of take-off/landing in vertical flight mode (VTOL) and flying over long distances in horizontal flight mode. Full dynamic model of the vehicle is derived using Newton-Euler formulation. Linear and nonlinear controllers for the stabilization of attitude of the vehicle and control of its altitude have been designed and implemented via simulations. In particular, an LQR controller has been shown to be quite effective in the vertical flight mode for all possible yaw angles. A sliding mode controller (SMC) with recursive nature has also been proposed to stabilize the vehicle's attitude and altitude. Simulation results show that proposed controllers provide satisfactory performance in achieving desired maneuvers.

Keywords—UAV, VTOL, dynamic model, stabilization, LQR, SMC

I. INTRODUCTION

Unmanned aerial vehicles (UAV) designed for various missions such as surveillance and exploration of disasters (fire, earthquake, flood, etc...) have been the subject of a growing research interest in the last decade. Airplanes with long flight ranges and helicopters with hovering capabilities constitute the major mobile platforms used in research of aerial vehicles. Besides these well known platforms, many researchers recently concentrate on the tilt rotor aerial vehicles combining the advantages of horizontal and vertical flight. Because these new vehicles have no conventional design basis, many research groups build their own tilt-rotor vehicles according to their desired technical properties and objectives. Some examples to these tilt-rotor vehicles are large scaled commercial aircrafts like Boeing's V22 Osprey [1], Bell's Eagle Eye [2] and smaller scale vehicles like Arizona State University's HARVee [3] and Compiègne University's BIROTAN [4] which consist of two rotors. Examples to other tilt-rotor vehicles with quad-rotor configurations are Boeing's V44 [5] (an ongoing project for the quad-rotor version of V22) and Chiba University's QTW UAV [6] which is a completed project.

Different controllers designed for the VTOL vehicles with quad-rotor configurations exist in the literature. Cranfield University's LQR controller [7], Swiss Federal Institute of Technology's PID and LQ controllers [8], Lakehead University's PD^2 [9] controller and Lund University's PID controller [13] are examples to the controller developed on quad-rotors linearized dynamic models. Among some other control methods of quad-rotor vehicles are CNRS

K. T. Oner, E. Cetinsoy, E. Sirimoglu, C. Hancer, T. Ayken and M. Unel are with Sabanci University, Orhanli-Tuzla, 34956, Istanbul TURKEY (corresponding author: munel@sabanciuniv.edu)

and Grenoble University's Global Stabilization [10], Swiss Federal Institute of Technology's Full Control of a Quadrotor [11] and Versailles Engineering Laboratory's Backstepping Control [12] that take into account the nonlinear dynamics of the vehicles.

In this paper we are presenting our current work on the modeling and control of a new tilt-wing aerial vehicle (SUAVI: Sabanci University Unmanned Aerial Vehicle) that is capable of flying in horizontal and vertical modes. The vehicle consists of four rotating wings and four rotors, which are mounted on leading edges of each wing.

The organization of this paper is as follows: In section II, full dynamic model of the vehicle is derived using Newton-Euler formulation. In section III, state-space controllers, a Linear Quadratic Regulator (LQR) and a Sliding Mode Controller (SMC) are developed.

Section IV gives the simulation results of the proposed control schemes. Section V concludes the paper with a discussion of future works.

II. DYNAMIC MODEL OF THE VEHICLE

The vehicle is equipped with four wings that are mounted on the front and at the back of the vehicle and can be rotated from vertical to horizontal positions. Fig. 1 below shows the aerial vehicle in various flight modes including the vertical (first one) and the horizontal (last one) flight modes.

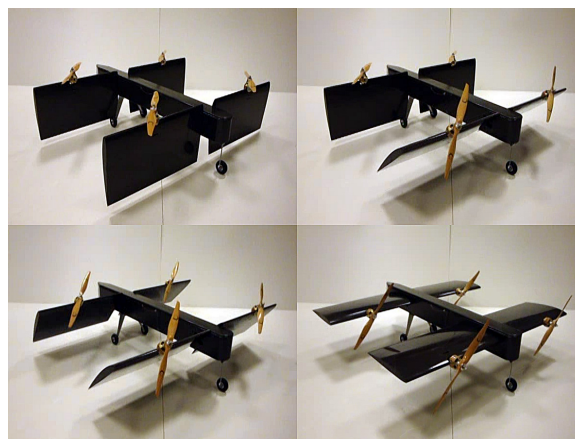


Fig. 1. SUAVI with integrated actuators in different flight configurations

With this wing configuration, the vehicle's airframe transforms into a quad-rotor like structure if the wings are at the vertical position and into an airplane like structure if the wings are at the horizontal position. To keep the control complexity on a minimum level, the rotations of the wings

are used as attitude control inputs in addition to motor thrust inputs in horizontal flight mode. Therefore the need for additional control surfaces that are put on trailing edges of the wings on a regular airplane are eliminated. Two wings on the front can be rotated independently to act like the ailerons while two wings at the back are rotated together to act like the elevator. This way the control surfaces of a regular plane in horizontal flight mode are mimicked with minimum number of actuators.

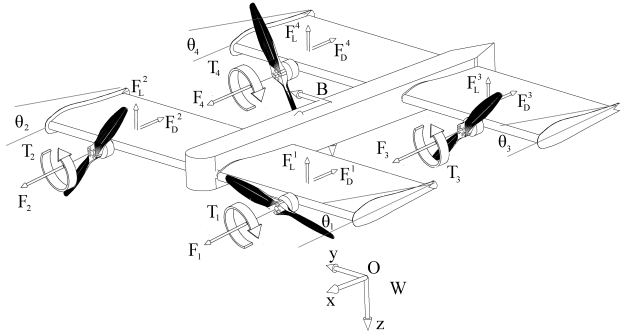


Fig. 2. Aerial Vehicle in a Tilted Configuration ($0 < \theta_i < \frac{\pi}{2}$)

The two reference frames given in Fig. 2 are body fixed reference frame $B : (O_b, x_b, y_b, z_b)$ and earth fixed inertial reference frame $W : (O_w, x_w, y_w, z_w)$. Using this model, the equations describing the position and attitude of the vehicle are obtained by relating the 6 DOF kinematic equations with the dynamic equations. The position and linear velocity of the vehicle's center of mass in world frame are described as,

$$P_w = \begin{bmatrix} X \\ Y \\ Z \end{bmatrix}, V_w = \dot{P}_w = \begin{bmatrix} \dot{X} \\ \dot{Y} \\ \dot{Z} \end{bmatrix}$$

The attitude and angular velocity of the vehicle in world frame are given as,

$$\alpha_w = \begin{bmatrix} \phi \\ \theta \\ \psi \end{bmatrix}, \Omega_w = \dot{\alpha}_w = \begin{bmatrix} \dot{\phi} \\ \dot{\theta} \\ \dot{\psi} \end{bmatrix}$$

where, ϕ , θ , ψ are named roll, pitch and yaw angles respectively. The equations for the transformation of the angular and linear velocities between world and body frames are given in equations (1) and (2):

$$V_b = \begin{bmatrix} v_x \\ v_y \\ v_z \end{bmatrix} = R(\phi, \theta, \psi) \cdot V_w \quad (1)$$

where

$$R(\phi, \theta, \psi) = R_z(\psi)R_y(\theta)R_x(\phi)$$

$$\Omega_b = \begin{bmatrix} p \\ q \\ r \end{bmatrix} = E(\phi, \theta) \cdot \Omega_w \quad (2)$$

$$E(\phi, \theta) = \begin{bmatrix} 1 & 0 & -s_\theta \\ 0 & c_\phi & s_\phi c_\theta \\ 0 & -s_\phi & c_\phi c_\theta \end{bmatrix}$$

The abbreviations s_β and c_β are used instead of $\sin(\beta)$ and $\cos(\beta)$ respectively.

The dynamic equations obtained for 6 DOF rigid body transformation of the aerial vehicle in inertial reference frame W are given as:

$$F_t = m\dot{V}_b + \Omega_b \times (m \cdot V_b) \quad (3)$$

$$M_t = I_b \dot{\Omega}_b + \Omega_b \times (I_b \cdot \Omega_b) \quad (4)$$

where m is the mass and the I_b is the inertia matrix expressed in the body frame B . The total force F_t acting on the vehicle's center of gravity is the sum of the forces F_{th} created by the rotors, the gravity F_g , the lift and drag forces generated by the wings F_w and the aerodynamic forces F_d which is considered as a disturbance, namely

$$F_t = F_g + F_w + F_{th} + F_d \quad (5)$$

where

$$F_g = \begin{bmatrix} -s_\theta \\ s_\phi c_\theta \\ c_\phi c_\theta \end{bmatrix} \cdot mg$$

and

$$F_w = \begin{bmatrix} (c_D(\theta_1, v_x, v_z) + c_D(\theta_2, v_x, v_z) + 2c_D(\theta_3, v_x, v_z)) \\ 0 \\ (c_L(\theta_1, v_x, v_z) + c_L(\theta_2, v_x, v_z) + 2c_L(\theta_3, v_x, v_z)) \end{bmatrix}$$

and

$$F_{th} = \begin{bmatrix} c_{\theta_1} + c_{\theta_2} + c_{\theta_3} + c_{\theta_4} \\ 0 \\ -s_{\theta_1} - s_{\theta_2} - s_{\theta_3} - s_{\theta_4} \end{bmatrix} \begin{bmatrix} k\omega_1^2 \\ k\omega_2^2 \\ k\omega_3^2 \\ k\omega_4^2 \end{bmatrix}$$

note that the propeller thrusts $F_{(1,2,3,4)}$ are modeled as:

$$F_i = k\omega_i^2$$

Because the wings at the back are rotated together their angle of attacks are the same for all time ($\theta_3 = \theta_4$). Note that the lift function $c_L(\theta_i, v_x, v_z)$ and the drag function $c_D(\theta_i, v_x, v_z)$ are not just functions of linear velocities (v_x and v_z) like on a fixed-wing type of an airplane, but also functions of angle of attack θ_i for each wing. The reader is referred to the Appendix for the explicit forms of these equations.

The total torque M_t acting on the vehicle's center of gravity is the sum of the torques M_{th} created by the rotors M_w created by the drag/lift forces of the wings, M_{gyro} created by the gyroscopic effects of the propellers and the aerodynamic torques M_d which is considered as a disturbance, namely

$$M_t = M_{gyro} + M_w + M_{th} + M_d \quad (6)$$

where

$$M_{gyro} = \sum_{i=1}^4 J[\eta_i \Omega_b \times \begin{bmatrix} c_{\theta_i} \\ 0 \\ -s_{\theta_i} \end{bmatrix} \omega_i]$$

$$\eta_{(1,2,3,4)} = 1, -1, -1, 1$$

Linearized state-space equation is given as:

and

$$M_w = \begin{bmatrix} (c_L(\theta_1, v_x, v_z) - c_L(\theta_2, v_x, v_z)) \\ (c_L(\theta_1, v_x, v_z) + c_L(\theta_2, v_x, v_z) - 2c_L(\theta_3, v_x, v_z)) \\ (-c_D(\theta_1, v_x, v_z) + c_D(\theta_2, v_x, v_z)) \end{bmatrix}$$

and

$$M_{th} = \begin{bmatrix} l_s s_{\theta_1} & -l_s s_{\theta_2} & l_s s_{\theta_3} & -l_s s_{\theta_3} \\ l_l s_{\theta_1} & l_l s_{\theta_2} & -l_l s_{\theta_3} & -l_l s_{\theta_3} \\ l_s c_{\theta_2} & -l_s c_{\theta_2} & l_s c_{\theta_3} & -l_s c_{\theta_3} \end{bmatrix} \begin{bmatrix} k\omega_1^2 \\ k\omega_2^2 \\ k\omega_3^2 \\ k\omega_4^2 \end{bmatrix} \\ + \begin{bmatrix} -c_{\theta_1} & -c_{\theta_2} & -c_{\theta_3} & -c_{\theta_3} \\ 0 & 0 & 0 & 0 \\ s_{\theta_1} & s_{\theta_2} & s_{\theta_3} & s_{\theta_3} \end{bmatrix} \begin{bmatrix} \lambda_1 k\omega_1^2 \\ \lambda_2 k\omega_2^2 \\ \lambda_3 k\omega_3^2 \\ \lambda_4 k\omega_4^2 \end{bmatrix}$$

Note that the sum of torques created by the rotors result in a roll moment along the x axis in horizontal flight mode ($\theta_{1,2,3} = 0$) and in a yaw moment along the z axis in vertical flight mode ($\theta_{1,2,3} = \pi/2$)

III. STATE-SPACE CONTROLLER DESIGN

To synthesize various controllers, equations derived in Section II are put into state-space form. The state vector χ consists of the position (P_w), the attitude (α_w), the linear velocity (V_b) and the angular velocity (Ω_b).

$$\chi = \begin{bmatrix} P_w \\ V_b \\ \Omega_b \\ \alpha_w \end{bmatrix} \quad (7)$$

In light of equations (1)-(6) we have

$$\dot{\chi} = \begin{bmatrix} \dot{P}_w \\ \dot{V}_b \\ \dot{\Omega}_b \\ \dot{\alpha}_w \end{bmatrix} = \begin{bmatrix} R^{-1}(\alpha_w) \cdot V_b \\ 1/m \cdot [F_t - \Omega_b \times (m \cdot V_b)] \\ I_b^{-1} \cdot [M_t - \Omega_b \times (I_b \cdot \Omega_b)] \\ E^{-1}(\alpha_w) \cdot \Omega_b \end{bmatrix} \quad (8)$$

which is a nonlinear plant of the form

$$\dot{\chi} = f(\chi, u) \quad (9)$$

Note that the aerial vehicle is an under-actuated system with 12 dimensional state vector and a 4 dimensional input vector.

A. Linearized System and LQR Controller Synthesis

For LQR controller design, the dynamic equations of the vehicle are linearized around nominal operating points in hovering condition. In the hovering mode, the controlled variables of the plant are chosen to be the position (X, Y, Z) and yaw angle (ψ). In order to simplify the controller design, the actuating forces and torques are decomposed into four virtual control inputs (u_i) as follows:

$$u = \begin{bmatrix} u_1 \\ u_2 \\ u_3 \\ u_4 \end{bmatrix} = \begin{bmatrix} -k(\omega_1^2 + \omega_2^2 + \omega_3^2 + \omega_4^2) \\ k l_s \cdot [(\omega_1^2 + \omega_3^2) - (\omega_2^2 + \omega_4^2)] \\ k l_l \cdot [(\omega_1^2 + \omega_2^2) - (\omega_3^2 + \omega_4^2)] \\ k(\lambda_1 \omega_1^2 + \lambda_2 \omega_2^2 + \lambda_3 \omega_3^2 + \lambda_4 \omega_4^2) \end{bmatrix} \quad (10)$$

$$\dot{\chi} = A\chi + Bu \quad (11)$$

Full yaw control is obtained by interpolating LQR controllers designed for certain number of nominal operating points.

B. Attitude and Altitude Stabilization via Sliding Mode Control (SMC)

The equations of motion for VTOL mode can be recast as:

$$\dot{\xi} = F(\xi) + B(\xi)u \quad (12)$$

where $\xi = [Z, \dot{Z}, \phi, \dot{\phi}, \theta, \dot{\theta}, \psi, \dot{\psi}]^T$ and $u = [u_1, u_2, u_3, u_4]^T$. Note that this equation is affine in input. Using this observation, it is possible to develop a sliding mode controller for the stabilization of the roll-pitch-yaw angles and vehicle's altitude. Let's define the sliding variable as:

$$\sigma = G\xi \quad (13)$$

where G is a 4×8 matrix such that (GB) is invertible. By differentiating σ one gets:

$$\dot{\sigma} = G\dot{\xi} = GF + GBu \quad (14)$$

Sliding mode control is given as:

$$u = u_{eq} - K \text{sgn}(\sigma) \quad (15)$$

where u_{eq} is the equivalent control, which is the continuous part of the control u , $\text{sgn}(\cdot)$ is the well-known signum function and $K > 0$. The equivalent control is obtained by setting $\dot{\sigma} = 0$, namely

$$\dot{\sigma} = GF + GBu_{eq} = 0 \Rightarrow u_{eq} = -(GB)^{-1}GF \quad (16)$$

However, computation of u_{eq} can be difficult since the exact knowledge of $F(\xi)$ and $B(\xi)$ are required. Below we will eliminate computation of u_{eq} using continuity of u_{eq} and obtain a recursive control law. Note that in light of (14) and (16) we have:

$$\dot{\sigma} = (GB)(u + (GB)^{-1}GF) = (GB)(u - u_{eq}) \quad (17)$$

Choosing a Lyapunov function $V = (1/2)\sigma^T \sigma \geq 0$, and differentiating with respect to time one gets:

$$\dot{V} = \sigma^T \dot{\sigma}, \quad (18)$$

where D is a positive-definite matrix. \dot{V} can be made negative-definite by selecting

$$\dot{\sigma} = -D\sigma \Rightarrow \dot{V} = -\sigma^T D\sigma \leq 0 \quad (19)$$

In light of (17) and (19), the following equations can be obtained:

$$\dot{\sigma} = (GB)(u - u_{eq}) \Rightarrow u - u_{eq} = (GB)^{-1}\dot{\sigma} \quad (20)$$

and

$$(GB)(u - u_{eq}) = -D\sigma \Rightarrow u - u_{eq} = -(GB)^{-1}D\sigma \quad (21)$$

Computing above equations at two different sampling instants, i.e. $t = (k-1)T$ and $t = kT$, namely

$$u((k-1)T) - u_{eq}((k-1)T) = (GB)^{-1} \dot{\sigma}((k-1)T) \quad (22)$$

$$u(kT) - u_{eq}(kT) = -(GB)^{-1} D\sigma(kT) \quad (23)$$

Since the equivalent control is continuous, we have

$$\lim_{\Delta \rightarrow 0} u_{eq}(t - \Delta) = u_{eq}(t) \quad (24)$$

Assuming that the sampling time is small (i.e. $T \approx \Delta$),

$$u_{eq}(kT) = u_{eq}((k-1)T) \quad (25)$$

Substituting (25) into (22) and (23), and approximating $\dot{\sigma}$ using Euler's backward difference one derives the following recursion for the control law:

$$u[k] = u[k-1] - (GB)^{-1} \left[\frac{(I+TD)\sigma[k] - \sigma[k-1]}{T} \right] \quad (26)$$

where I is the identity matrix and $[k]$ denotes (kT) . This control is implemented to achieve roll-pitch-yaw stabilization and altitude control for hovering operation. Once the controller takes the vehicle into a desired altitude, tilt wing transition is then carried out which is given in the following section.

IV. SIMULATION RESULTS

The performance of the LQR controller is evaluated on the nonlinear dynamic model of the vehicle given by (8) in MATLAB/Simulink. Q and R matrices used in LQR design are selected as $Q = 10^{-1} \cdot I_{12 \times 12}$ and $R = \text{diag}(10^{-1}, 10, 10, 10)$

Starting with the initial configuration $P_w = (0, 0, 0)^T$ and $\alpha_w = (0, 0, 0)^T$ of the vehicle, the simulation results given in Fig. 3 and Fig. 4 show the variation of the position and attitude variables for the reference inputs $P_{ref} = (5, -5, -10)^T$ and $\psi_r = \pi/2$ under random disturbance.

Note that position and angle references are tracked with negligible steady state errors. The lift forces generated by each rotor are shown in Fig. 5.

It is important to note that the control effort is small and the magnitude of the forces that need to be generated don't exceed the physical limits (≈ 16 N) of the rotors and remain in the $\pm 20\%$ margin of nominal thrust.

A 3D visualization environment in MATLAB using VR tool has been developed to visualize maneuvers of the aerial vehicle in 3D space. Result of applying LQR control is depicted in Fig. 6.

The sliding mode controller performed very good in tracking the reference inputs. Fig. 7 and Fig. 8 show the response of sliding mode controller in tracking the desired references. Note that, even though the reference angles are relatively large (i.e. 0.5 rad), the controller reaches the desired roll and pitch angles within almost 1 second. The sluggish response in yaw movement is due to the nature of the actuation. Moreover, even though the altitude response is almost as fast as LQR controller, the sliding mode control of altitude has almost zero overshoot in comparison to LQR. Fig. 9 shows the control effort of sliding mode control.

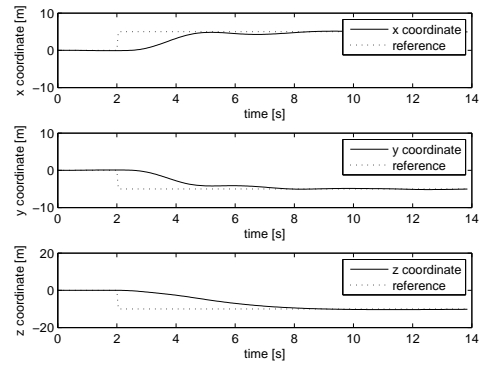


Fig. 3. Position control of the vehicle using LQR

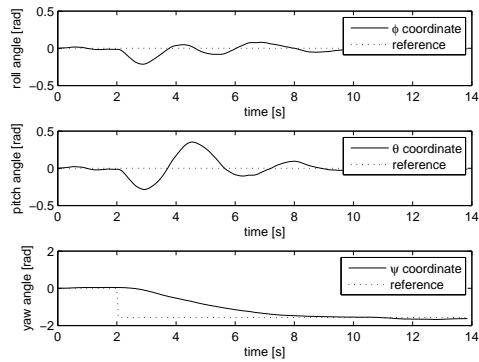


Fig. 4. Attitude control of the vehicle using LQR

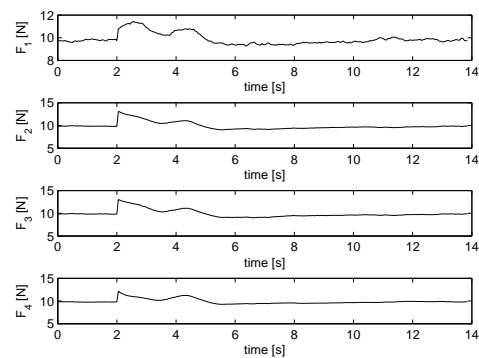


Fig. 5. Forces generated by the motors

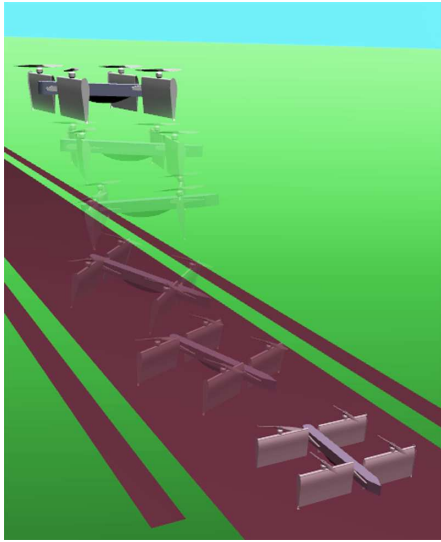


Fig. 6. Visualization of Position and Heading Control Results of LQR

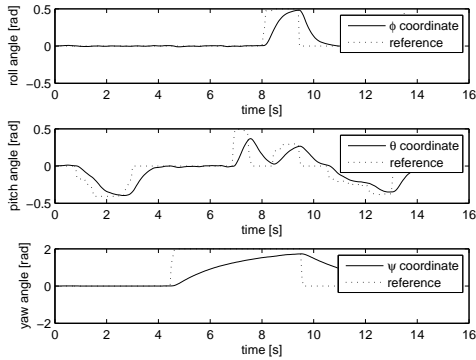


Fig. 7. Attitude Control Using Sliding Mode Controller

V. CONCLUSION AND FUTURE WORKS

In this paper we have reported our ongoing work on modeling and control of a new tilt-wing aerial vehicle (SUAVI). The full dynamic model of the vehicle is derived using Newton-Euler formulation. An LQR based position control algorithm is developed and applied to the nonlinear dynamic model of the vehicle in vertical flight mode. A good position tracking performance is obtained using this controller. Furthermore, a sliding mode controller with recursive implementation is tested to provide the attitude and altitude stability of the vehicle. Results show that the proposed method performs good tracking of the desired attitude and altitude. Future work will include improvements on the controller synthesis. Experiments will be performed on the actual vehicle.

VI. ACKNOWLEDGMENTS

Authors would like to acknowledge the support provided by TUBITAK (The Scientific and Technological Research Council of Turkey) under grant 107M179.

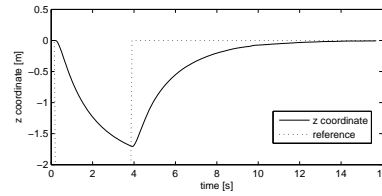


Fig. 8. Altitude Control Using Sliding Mode Controller

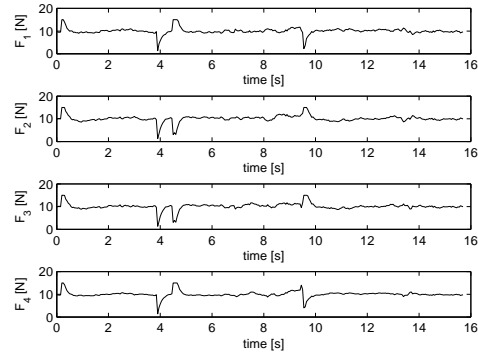


Fig. 9. Control Effort in Sliding Mode Controller

VII. APPENDIX

The drag and lift forces created by the wings are modeled using the data obtained from ANSYS® simulations.

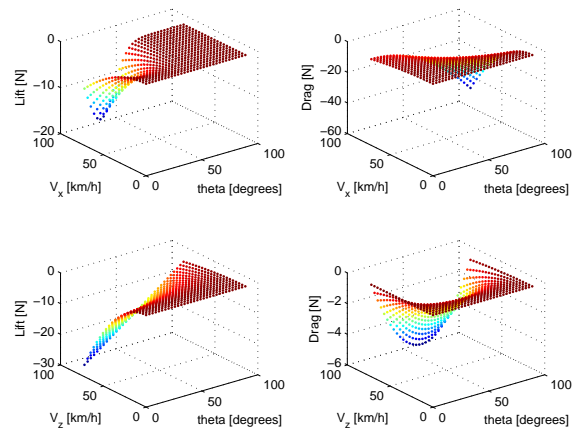


Fig. 10. The Lift and Drag Forces Created by the Wings

$$c_D = -\frac{(2.4 + 10\theta^2)}{256} |V_x| V_x - \frac{(-5(\pi/4 - \theta)^2 + 3.0842)}{256} |V_z| V_z$$

$$c_L = -\frac{9.81e^{-(\frac{\theta-0.3}{0.6})^2}}{256} |V_x| V_x - \frac{(1 + 10(\pi/2 - \theta))}{256} |V_z| V_z$$

REFERENCES

- [1] Boeing, V-22 Osprey, September 13, 2008.
<http://www.boeing.com/rotorcraft/military/v22/index.htm>
- [2] The Bell Eagle Eye UAS, September 13, 2008.
<http://www.bellhelicopter.com/en/aircraft/military/bellEagleEye.cfm>
- [3] J.J. Dickeson, D. Miles, O. Cifdaloz, Wells, V.L. Rodriguez, A.A., "Robust LPV H Gain-Scheduled Hover-to-Cruise Conversion for a Tilt-Wing Rotorcraft in the Presence of CG Variations," *American Control Conference. ACC '07*, vol., no., pp.5266-5271, 9-13 July 2007
- [4] F. Kendoul, I. Fantoni, R. Lozano, "Modeling and control of a small autonomous aircraft having two tilting rotors," *Proceedings of the 44th IEEE Conference on Decision and Control, and the European Control Conference*, December 12-15, Seville, Spain, 2005
- [5] Snyder, D., "The Quad Tiltrotor: Its Beginning and Evolution," Proceedings of the 56th Annual Forum, *American Helicopter Society*, Virginia Beach, Virginia, May 2000.
- [6] K. Nonami, "Prospect and Recent Research & Development for Civil Use Autonomous Unmanned Aircraft as UAV and MAV," *Journal of System Design and Dynamics*, Vol.1, No.2, 2007
- [7] I. D. Cowling, O. A. Yakimenko, J. F. Whidborne and A. K. Cooke, "A Prototype of an Autonomous Controller for a Quadrotor UAV," *European Control Conference 2007* Kos, 2-5 July, Kos, Greek, 2007.
- [8] S. Bouabdallah, A. Noth and R. Siegwart, "PID vs LQ Control Techniques Applied to an Indoor Micro Quadrotor," *Proc. of 2004 IEEE/RSJ Int. Conference on Intelligent Robots and Systems*, September 28 - October 2, Sendai, Japan, 2004.
- [9] A. Tayebi and S. McGilvray, "Attitude Stabilization of a Four-Rotor Aerial Robot" *43rd IEEE Conference on Decision and Control*, December 14-17 Atlantis, Paradise Island, Bahamas, 2004.
- [10] A. Hably and N. Marchand, "Global Stabilization of a Four Rotor Helicopter with Bounded Inputs", *Proc. of the 2007 IEEE/RSJ Int. Conference on Intelligent Robots and Systems*, Oct 29 - Nov 2, San Diego, CA, USA, 2007
- [11] S. Bouabdallah and R. Siegwart, "Full Control of a Quadrotor ", *Proc. of the 2007 IEEE/RSJ Int. Conference on Intelligent Robots and Systems*, Oct 29 - Nov 2, San Diego, CA, USA, 2007.
- [12] Tarek Madani and Abdelaziz Benallegue, "Backstepping Control for a Quadrotor Helicopter ", *Proc. of the 2006 IEEE/RSJ Int. Conference on Intelligent Robots and Systems*, October 9 - 15, Beijing, China, 2006.
- [13] Tommaso Bresciani, "Modeling Identification and Control of a Quadrotor Helicopter ", *Master Thesis, Department of Automatic Control, Lund University*, October, 2008.